Quantum cascade lasers: from tool to product

M. Razeghi,* Q. Y. Lu, N. Bandyopadhyay, W. Zhou, D. Heydari, Y. Bai, and S. Slivken

Center for Quantum Devices, Department of Electrical Engineering and Computer Science, Northwestern University, Evanston, Illinois 60208, USA

razeghi@eecs.northwestern.edu

Abstract: The quantum cascade laser (QCL) is an important laser source in the mid-infrared and terahertz frequency range. The past twenty years have witnessed its tremendous development in power, wall plug efficiency, frequency coverage and tunability, beam quality, as well as various applications based on QCL technology. Nowadays, QCLs can deliver high continuous wave power output up to 5.1 W at room temperature, and cover a wide frequency range from 3 to 300 μm by simply varying the material components. Broadband heterogeneous QCLs with a broad spectral range from 3 to 12 μm, wavelength agile QCLs based on monolithic sampled grating design, and on-chip beam QCL combiner are being developed for the next generation tunable mid-infrared source for spectroscopy and sensing. Terahertz sources based on nonlinear generation in QCLs further extend the accessible wavelength into the terahertz range. Room temperature continuous wave operation, high terahertz power up to 1.9 mW, and wide frequency tunability form 1 to 5 THz makes this type of device suitable for many applications in terahertz spectroscopy, imaging, and communication.

OCIS codes: (140.3070) Infrared and far-infrared lasers; (140.5965) Semiconductor lasers, quantum cascade; (230.5590) Quantum-well, -wire and -dot devices; (140.3490) Lasers, distributed-feedback; (190.4223) Nonlinear wave mixing.

References and links

1. R. Kazarinov and R. A. Suris, "Possibility of amplication of electromagnetic waves in a semiconductor with a superlattice," Sov. Phys. Semicond. **5**, 707–709 (1971).
2. J. Faist, F. Capasso, D. L. Sivco, C. Sirtori, A. L. Hutchinson, and A. Y. Cho, "Quantum cascade laser," Science **264**(5158), 553–556 (1994).
3. M. Razeghi, "High-performance InP-based mid-IR quantum cascade lasers," IEEE J. Quantum Electron. **15**(3), 941–951 (2009).
4. Y. Yao, A. J. Hoffman, and C. F. Gmachl, "Mid-infrared quantum cascade lasers," Nat. Photonics **6**(7), 432–439 (2012).
5. C. Sirtori, S. Barbieri, and R. Colombelli, "Wave engineering with THz quantum cascade lasers," Nat. Photonics **7**(9), 691–701 (2013).
6. R. F. Curl, F. Capasso, C. Gmachl, A. A. Kosterev, B. McManus, R. Lewicki, M. Pusharsky, G. Wysocki, and F. K. Tittel, "Quantum cascade lasers in chemical physics," Chem. Phys. Lett. **487**(1-3), 1–18 (2010).
7. M. Razeghi, *The MOCVD Challenge: A survey of GaInAsP-InP and GaInAsP-GaAs for Photonic and Electronic Device Applications, Electronic Materials and Devices*, ed.II, (CRC, 2010).
8. M. Razeghi, *Technology of Quantum Devices* (Springer Science, 2010).
9. Y. Bai, N. Bandyopadhyay, S. Tsao, S. Slivken, and M. Razeghi, "Room temperature quantum cascade lasers with 27% wall plug efficiency," Appl. Phys. Lett. **98**(18), 181102 (2011).
10. Y. Bai, S. Tsao, N. Bandyopadhyay, S. Slivken, Q. Y. Lu, D. Caffey, M. Pushkarsky, T. Day, and M. Razeghi, "High power, continuous wave, quantum cascade ring laser," Appl. Phys. Lett. **99**(26), 261104 (2011).
11. Y. Bai, S. Slivken, Q. Y. Lu, N. Bandyopadhyay, and M. Razeghi, "Angled cavity broad area quantum cascade lasers," Appl. Phys. Lett. **100**(8), 081106 (2012).
12. M. Beck, D. Hofstetter, T. Aellen, J. Faist, U. Oesterle, M. Ilegems, E. Gini, and H. Melchior, "Continuous Wave Operation of a Mid-Infrared Semiconductor Laser at Room Temperature," Science **295**(5553), 301–305 (2002).
13. J. S. Yu, A. Evans, S. Slivken, S. R. Darvish, and M. Razeghi, "Temperature dependent characteristics of λ ~ 3.8 μm room-temperature continuous-wave quantum-cascade lasers," Appl. Phys. Lett. **88**(25), 251118 (2006).

#229245 - $15.00 USD Received 8 Dec 2014; revised 7 Jan 2015; accepted 27 Jan 2015; published 25 Mar 2015

14. S. Slivken, A. Evans, W. Zhang, and M. Razeghi, "High-power, continuous-operation intersubband laser for wavelengths greater than 10μm," Appl. Phys. Lett. **90**(15), 151115 (2007).
15. A. Evans, J. S. Yu, S. Slivken, and M. Razeghi, "Continuous-wave operation of λ~4.8μm quantum-cascade lasersat room temperature," Appl. Phys. Lett. **85**(12), 2166–2168 (2004).
16. Y. Bai, N. Bandyopadhyay, S. Tsao, E. Selcuk, S. Slivken, and M. Razeghi, "Highly temperature insensitive quantum cascade lasers," Appl. Phys. Lett. **97**(25), 251104 (2010).
17. Y. Bai, S. Slivken, S. Kuboya, S. R. Darvish, and M. Razeghi, "Quantum cascade lasers that emit more light than heat," Nat. Photonics **4**(2), 99–102 (2010).
18. P. Q. Liu, A. J. Hoffman, M. D. Escarra, K. J. Franz, J. B. Khurgin, Y. Dikmelik, X. Wang, J.-Y. Fan, and C. F. Gmachl, "Highly power-efficient quantum cascade lasers," Nat. Photonics **4**(2), 95–98 (2010).
19. Q. Y. Lu, Y. Bai, N. Bandyopadhyay, S. Slivken, and M. Razeghi, "Room-temperature continuous wave operation of distributed feedback quantum cascade lasers with watt-level power output," Appl. Phys. Lett. **97**(23), 231119 (2010).
20. Q. Y. Lu, Y. Bai, N. Bandyopadhyay, S. Slivken, and M. Razeghi, "2.4W room temperature continuous wave operation of distributed feedback quantum cascade lasers," Appl. Phys. Lett. **98**(18), 181106 (2011).
21. W. W. Bewley, C. L. Canedy, C. S. Kim, M. Kim, C. D. Merritt, J. Abell, I. Vurgaftman, and J. R. Meyer, "High-power room-temperature continuous-wave mid-infrared interband cascade lasers," Opt. Express **20**(19), 20894–20901 (2012).
22. M. Razeghi, N. Bandyopadhyay, Y. Bai, Q. Y. Lu, and S. Slivken, "Recent advances in mid infrared (3-5 μm) Quantum Cascade Lasers," Opt. Mater. Express **3**(11), 1872–1884 (2013).
23. A. Bismuto, S. Riedi, B. Hinkov, M. Beck, and J. Faist, "Sb-free quantum cascade lasers in the 3 μm spectral range," Semicond. Sci. Technol. **27**(4), 045013 (2012).
24. N. Bandyopadhyay, Y. Bai, B. Gokden, A. Myzaferi, S. Tsao, S. Slivken, and M. Razeghi, "Watt level performance of quantum cascade lasers in room temperature continuous wave operation at λ~ 3.76 μm," Appl. Phys. Lett. **97**(13), 131117 (2010).
25. N. Bandyopadhyay, S. Slivken, Y. Bai, and M. Razeghi, "High power continuous wave, room temperature operation of λ~3.4 μm and λ~3.55 μm InP-based qantum cascade lasers," Appl. Phys. Lett. **100**(21), 212104 (2012).
26. N. Bandyopadhyay, Y. Bai, S. Tsao, S. Nida, S. Slivken, and M. Razeghi, "Room temperature continuous wave operation of λ ~ 3-3.2 μm quantum cascade lasers," Appl. Phys. Lett. **101**(24), 241110 (2012).
27. C. Gmachl, D. L. Sivco, R. Colombelli, F. Capasso, and A. Y. Cho, "Ultra-broadband semiconductor laser," Nature **415**(6874), 883–887 (2002).
28. A. Hugi, R. Terazzi, Y. Bonetti, A. Wittmann, M. Fischer, M. Beck, J. Faist, and E. Gini, "External cavity quantum cascade laser tunable from 7.6 to 11.4 μm," Appl. Phys. Lett. **95**(6), 061103 (2009).
29. N. Bandyopadhyay, Y. Bai, S. Slivken, and M. Razeghi, "High power operation of λ ~ 5.2–11 μm strain balanced quantum cascade lasers based on the same material composition," Appl. Phys. Lett. **105**(7), 071106 (2014).
30. S. Slivken, N. Bandyopadhyay, S. Tsao, S. Nida, Y. Bai, Q. Y. Lu, and M. Razeghi, "Sampled grating, distributed feedback quantum cascade lasers with a broad tunability and continuous wave operation at room temperature," Appl. Phys. Lett. **100**(26), 261112 (2012).
31. S. Slivken, N. Bandyopadhyay, S. Tsao, S. Nida, Y. Bai, Q. Y. Lu, and M. Razeghi, "Dual Section Quantum Cascade Lasers with Wide Electrical Tuning," Proc. SPIE **8631**, 86310P (2013).
32. S. Slivken, N. Bandyopadhyay, Y. Bai, Q. Y. Lu, and M. Razeghi, "Extended electrical tuning of quantum cascade lasers with digital concatenated gratings," Appl. Phys. Lett. **103**(23), 231110 (2013).
33. B. G. Lee, M. Belkin, C. Pflugl, L. Diehl, H. A. Zhang, R. M. Audet, J. MacArthur, D. Bour, S. Corzine, G. Hofler, and F. Capasso, "Distributed feedback quantum cascade laser arrays," IEEE J. Quantum Electron. **45**, 554–565 (2009).
34. L. K. Hoffmann, M. Klinkmüller, E. Mujagić, M. P. Semtsiv, W. Schrenk, W. T. Masselink, and G. Strasser, "Tree array quantum cascade laser," Opt. Express **17**(2), 649–657 (2009).
35. W. Zhou, S. Slivken, N. Bandyopadhyay, Y. Bai, Q. Y. Lu, and M. Razeghi, "Wide electrical tunable quantum cascade lasers array with on-chip beam combiner," under preparation (2014).
36. M. A. Belkin, F. Capasso, A. Belyanin, D. L. Sivco, A. Y. Cho, D. C. Oakley, C. J. Vineis, and G. W. Turner, "Terahertz quantum-cascade-laser source based on intracavity difference-frequency generation," Nat. Photonics **1**(5), 288–292 (2007).
37. M. A. Belkin, F. Capasso, F. Xie, A. Belyanin, M. Fischer, A. Wittmann, and J. Faist, "Room temperature terahertz quantum cascade laser source based on intracavity difference-frequency generation," Appl. Phys. Lett. **92**(20), 201101 (2008).
38. Q. Y. Lu, N. Bandyopadhyay, S. Slivken, Y. Bai, and M. Razeghi, "Room temperature single-mode terahertz sources based on intracavity difference- frequency generation in quantum cascade lasers," Appl. Phys. Lett. **99**(13), 131106 (2011).
39. M. Razeghi, Q. Y. Lu, N. Bandyopadhyay, Y. Bai, and S. Slivken, "Recent progress of room temperature THz sources based on nonlinear frequency mixing in quantum cascade lasers," Proc. SPIE **9100**, 910016 (2014).
40. Q. Y. Lu, N. Bandyopadhyay, S. Slivken, Y. Bai, and M. Razeghi, "High performance terahertz quantum cascade laser sources based on intracavity difference frequency generation," Opt. Express **21**(1), 968–973

#229245 - $15.00 USD Received 8 Dec 2014; revised 7 Jan 2015; accepted 27 Jan 2015; published 25 Mar 2015

(2013).
41. K. Vijayraghavan, R. W. Adams, A. Vizbaras, M. Jang, C. Grasse, G. Boehm, M. C. Amann, and M. A. Belkin, "Terahertz Sources Based on Čerenkov Difference-Frequency Generation in Quantum Cascade Lasers," Appl. Phys. Lett. **100**(25), 251104 (2012).
42. Q. Y. Lu, N. Bandyopadhyay, S. Slivken, Y. Bai, and M. Razeghi, "Widely tuned room temperature terahertz quantum cascade laser sources based on difference-frequency generation," Appl. Phys. Lett. **101**(25), 251121 (2012).
43. Q. Y. Lu, N. Bandyopadhyay, S. Slivken, Y. Bai, and M. Razeghi, "Room temperature terahertz quantum cascade laser sources with 215 μW output power through epilayer-down mounting," Appl. Phys. Lett. **103**(1), 011101 (2013).
44. M. Razeghi, Q. Y. Lu, N. Bandyopadhyay, Y. Bai, and S. Slivken, "Room temperature continuous wave THz quantum cascade laser source with high power operation," Proc. SPIE **9199**, 919902 (2014).
45. B. Gokden, Y. Bai, N. Bandyopadhyay, S. Slivken, and M. Razeghi, "Angled cavity broad area quantum cascade lasers," Appl. Phys. Lett. **97**, 131112 (2010).
46. Q. Y. Lu, N. Bandyopadhyay, S. Slivken, Y. Bai, and M. Razeghi, "Continuous operation of a monolithic semiconductor terahertz source at room temperature," Appl. Phys. Lett. **104**(22), 221105 (2014).
47. Q. Y. Lu, S. Slivken, N. Bandyopadhyay, Y. Bai, and M. Razeghi, "Widely tunable room temperature semiconductor terahertz source," Appl. Phys. Lett. **105**(20), 201102 (2014).

1. Introduction

Since the invention of lasers in the 1960s, people have been consistently pursuing a laser source that is smaller, cheaper, higher power, and more wavelength agile. As a semiconductor laser, the quantum cascade laser (QCL) is an energy-band engineered device where the electromagnetic radiation is achieved by intersubband transitions between energy levels inside superlattice quantum wells [1]. Since the first experimental demonstration in 1994 [2], QCL technology has undergone tremendous development. These performance levels are the result of constant improvement in the structure design, material quality, and fabrication technology [3–5]. Nowadays, it is becoming the leading laser source in the mid-infrared (mid-IR) and terahertz (THz) frequency ranges, and has many applications in gas sensing, environmental monitoring, medical diagnosis, security and defense [6].

The Center for Quantum Devices (CQD) at Northwestern University was built with the goal of advancing optoelectronic technology, from the UV to the THz spectral regions. This includes development of many different technologies based on III-V semiconductors [7, 8]. Since 1997, the CQD has put considerable effort into the development of the QCL, especially with regard to power, wall plug efficiency (WPE), single mode operation, tuning, and beam quality, pushing the QCL from a laboratory tool to a widespread product benefiting the general public. We have demonstrated the most efficient and most powerful QCL in room temperature continuous wave operation with 21% WPE and 5.1 W output power [9], room temperature continuous wave operation of ring cavity surface emitting QCL with 0.51 W output power [10], and the first β-type distributed feedback QCL [11]. In this paper, we present some of our recent breakthroughs in QCLs, discussed in detail in the following sections, on high power high efficiency QCLs; high performance QCLs at λ~3-4 μm; broadband QCLs at λ~6-10 μm, wavelength agile QCLs; QCLs with on-chip beam combining for wide electrical tuning; and THz sources based on difference frequency generation (DFG) in mid-IR QCLs.

2. High power and high efficiency quantum cascade laser

Eight years after the invention of the QCL, the first room temperature CW QCL was demonstrated at 9.1 μm with an output power of 10 mW [12]. Shortly after that, CQD at Northwestern University demonstrated high power room temperature cw operation across a wide range of wavelength from 3.8 μm [13] to 10.6 μm [14]. Since 2007, concentrated effort has been put on wavelengths around 4.7 μm, which is attractive for infrared countermeasures, free space communication, chemical sensing applications, etc. At that time, the best reported room temperature cw power around this wavelength was 0.3 W with a WPE of 3.7% [15]. By 2011, QCL reached an output power of 5.1 W with a WPE of 21% in room temperature cw

#229245 - $15.00 USD Received 8 Dec 2014; revised 7 Jan 2015; accepted 27 Jan 2015; published 25 Mar 2015

operation [9]. In room temperature pulsed mode operation, the WPE increased from 7.7% to 27%. This trend is shown in Fig. 1(a).

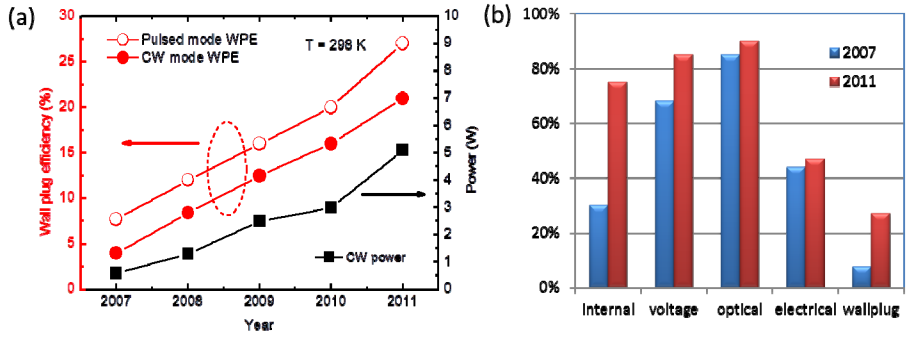

Fig. 1. (a) QCL performance improvement from 2007 to 2011. (b) Comparison of the sub-efficiencies and the wall plug efficiency in 2007 and 2011.

In general, a higher WPE leads to a higher output power. Our strategy of achieving the highest WPE in room temperature continuous wave operation can be divided in two parts. On one hand, we demonstrate the highest WPE at room temperature in pulsed mode operation. This is mostly design and material wise for the gain medium. On the other hand, we take the thermal consideration throughout the design and processing of the device, intending to achieve the highest thermal conductance, in which case the CW WPE can be brought closest to the corresponding pulsed WPE. The pulsed wall plug efficiency can be decomposed into four sub-efficiencies, i.e., the internal quantum efficiency, voltage efficiency, electrical efficiency, and optical efficiency. Out of the 4 sub-efficiencies, the internal quantum efficiency is the most important one and it can only be improved by exploring the design of the core structures [16]. Figure 1(b) shows that the internal quantum efficiency experienced the largest improvement. The most advanced room temperature QCL design is the shallow-well design reported in [16]. For room temperature cw operation, the best results are obtained with buried ridge regrowth and epilayer-down bonding. In addition, the ridge width of the buried ridge structure is also very important. A compromise needs to be made for low loss and high thermal conductance. Detailed discussion can be found in [3].

WPE is an important figure of merit representing the overall quality of the device. Despite impressive progress made in the past few years, further improving the WPE always stands a tremendous challenge. It would be interesting to see whether 50% WPE can be realized if the temperature constraint is removed. 50% is an important mile stone because it marks the winning of photon generation against phonon generation. In order to meet this challenge, two new designs were specifically made for low temperature high efficiency operation, termed as the single-well-injector design [17] and 'ultrastrong coupling' active design [18]. The uniqueness of the single-well-injector design is found in its injector state. Originating from a single injector well, there is only one injector state in this structure. The spatial and energetic location of this injector state is carefully engineered so that at the turn-on condition a "thermal forward filling" scheme is established. This scheme is advantageous for population inversion and carrier transport. As such, the internal quantum efficiency and the voltage efficiency are maximized. With this structure, a WPE of 53% is demonstrated, which represents the highest value for any QCL.

Over the years, several important breakthroughs have been demonstrated around a particular wavelength of 4.7 μm. Most of these breakthroughs can be easily adapted to other mid-infrared wavelengths as well. Out of everything, the material quality is of primary importance and strongly influences both the differential gain and transport within the device.

#229245 - $15.00 USD Received 8 Dec 2014; revised 7 Jan 2015; accepted 27 Jan 2015; published 25 Mar 2015

Though significant effort has been devoted to improving material quality, interface roughness still exists. At present, many of the "optimized" designs presented are simply reacting to the material that currently exists within each research group. Changes in transport coherence resulting from interface effects are a prime example, and can change peak current through a tunneling device dramatically. As such, while some improvements are still expected by fine tuning oscillator strengths and anticrossing energies, the real key to improving device performance will be material-based.

Thanks to the rapid development of high-efficiency QCLs, room temperature CW operation DFB QCLs with high power has been realized at λ~4.6-4.8 μm [19, 20]. A simple surface grating with a grating depth of 120 nm was designed and fabricated. The calculated coupling coefficient of 1.37cm^{-1} and modal loss discrimination of 0.4 cm^{-1} was sufficient for the single mode operation of a 5 mm long cavity. The back facet was HR coated, while the front facet was Anti reflection (AR) coated. The AR coating not only helps to enhance the slope efficiency, but also contribute to purify the lasing spectrum with higher mirror loss to the FP modes. The 11 μm wide and 5 mm long DFB QCL device generated 2.4 W output power at RT, CW condition with 10% WPE. Single mode emission with side mode suppression ration (SMSR) of 30 dB and single lobed far field in the entire current range was observed.

3. High performance QCLs at λ~3-4 μm

Many fundamental C-H, N-H, and O-H stretching modes have strong resonances in the 3-4 μm electromagnetic spectrum range. For example, methane, formaldehyde, carbon monoxide, and nitrous oxide which are strong greenhouse gases. Hence these fingerprint regions are particularly interesting for applications like pollution control, breath analysis, or detection of water contaminants. As a result, an efficient source of radiation within this wavelength range is essential in spectroscopic detection of trace gases. Interband cascade lasers (ICLs) present good sources for the short wavelength region due to low threshold current densities and high output power [21]. QCLs are also suitable sources in this spectral range due to the high power and unique possibility to tailor the emission frequency [22,23].

One of the ways to implement 3-4 μm QCLs is to apply the knowledge of QCLs obtained from the higher wavelength side of 4-5 μm. Similar to its longer wavelength counterpart, 3 well active region or single phonon resonance was used to design the active region since in comparison to double phonon resonance or bound to continuum designs, the upper laser level is lower down in terms of absolute energy in the quantum well system. This creates better confinement of electrons and increases the activation energy of electron escape through optical phonon emission and thermal emission to the continuum.

The key to the 3-4 μm QCL is the highly strain-balanced superlattice $Ga_xIn_{1-x}As$/ $Al_yIn_{1-y}As$ with high material quality [22]. As the wavelength becomes shorter, the emitting photon energy gets higher, and a higher strain is necessary to provide sufficient energy confinement for the electrons. From 4 to 5 μm to 3-4 μm, the Ga component in the GaInAs wells was increased from 31% to 21%, the Al component in the AlInAs barriers was increased from 64% to 89%. As a result, the conduction band offset was enhanced from 0.8 eV to 1.2 eV [24–26].

The growth of this highly strain-balanced superlattice is very challenging. We use gas-source molecular beam epitaxy (GSMBE) of custom design to grow our structure on n-InP substrate. The GSMBE reactor is dedicated exclusively for the QCL growth. The reactor is regularly maintained to ensure consistent high material quality. Postgrowth characterizations are performed for each growth to confirm the design parameters and monitor the growth conditions. The layer thickness and composition are characterized by SEM and high resolution X-ray diffraction. The experimental and simulated (X' Pert Epitaxy) x-ray diffraction curves for the laser core are shown in Fig. 2. Excellent agreement has been found between the two curves, confirming the material compositions. The increase in strain in the

#229245 - $15.00 USD Received 8 Dec 2014; revised 7 Jan 2015; accepted 27 Jan 2015; published 25 Mar 2015

superlattice was accompanied by sharp interface as was determined by low background and sharp higher order superlattice peaks in x-ray, with the smallest full width at half maximum (FWHM) of the satellite peak being 21.2 arc sec.

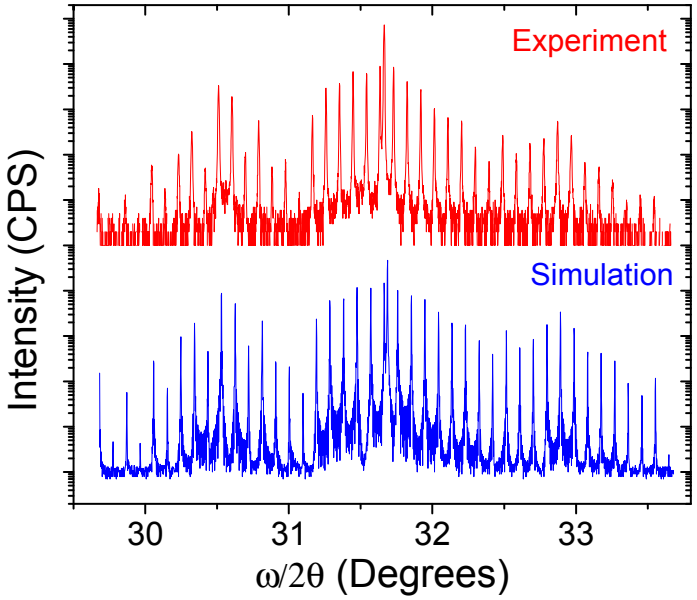

Fig. 2. Experimental and simulated x-ray diffraction curve of a 30-stage laser core.

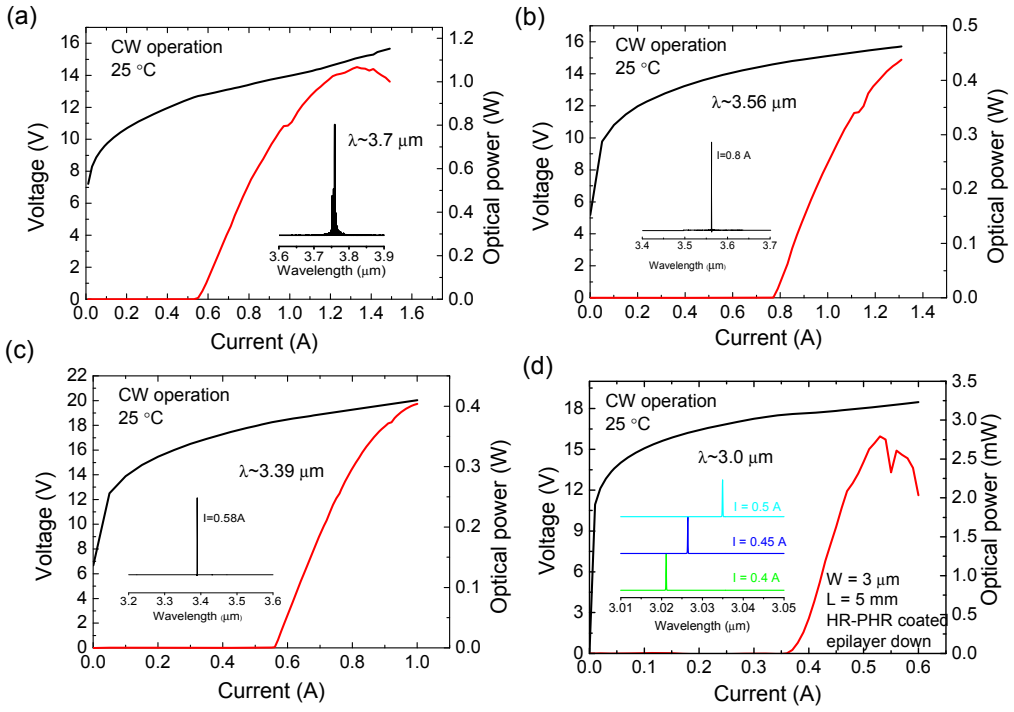

Fig. 3. P-I-V performances of QCLs in the 3-4 μm wavelength range.

In the past few years, a series of experiments were performed to shorten QCL emitting wavelength. To achieve room temperature CW operation with high power, the wafers were

#229245 - $15.00 USD Received 8 Dec 2014; revised 7 Jan 2015; accepted 27 Jan 2015; published 25 Mar 2015

processed into a buried ridge geometry with ridge widths ranging 3-10 μm. A device with cavity length of 3-5 mm was cleaved and epi-down mounted on a diamond submount. Figure 3 summarizes the power-current-voltage (*P-I-V*) performance development of QCLs from 3.7 to 3.0 μm. At λ~3.7 μm, the maximum RT, CW output power was 1.1W, with a threshold current density of 1.67KA/cm^2 and slope efficiency near threshold of 2.16 W/A. A maximum RT, WPE of 6% and 10% was obtained in CW and pulsed operation, respectively. In the 3.3-3.6 μm range, maximum RT, CW powers of 437 mW and 403mW were obtained at λ~3.56 μm and λ~3.39 μm respectively. At λ~3.7 μm QCL having a ridge width and cavity length of 3 μm and 5mm, respectively, shows a maximum CW output power of 2.8 mW at room temperature. The 3.02 μm emission is the shortest wavelength demonstration of CW operation at RT, for any QCL.

4. Broadband QCLs at λ~6-10 μm

The spectroscopic region between 5 and 11 μm is particularly rich in absorption lines of gases like NO, CH_4, N_2O, CO_2, NH_3, etc. To realize the full range mid-infrared spectroscopy, a broadly tunable source, without any gap in the spectrum, is required. This can be achieved by cascading multiple QCL cores, i.e. heterogeneous active structure [27], with peak gains at different wavelengths, to form a broad and flat gain spectrum, where individual wavelengths can be selected by an optical feedback mechanism. Previously, the active regions were designed in lattice matched $Al_{0.48}In_{0.52}As/Ga_{0.47}In_{0.53}As$ so that a very thick broadband structure comprising of many cores can be grown without strain relaxation [28]. While this was successful for longer wavelength emission, the performance of lattice matched QCLs deteriorates at shorter wavelength [4]. Strain balanced structures can solve this problem, but the strain levels, hence material compositions, are usually changing with emission wavelength due to the difference in well and barrier widths. Changing the composition dynamically during a single growth run in a standard MBE reactor by changing the effusion cell temperatures would lead to uncertainty in the growth rates and composition. This would lead to uncertainty in the emission wavelengths of individual cores, and prevent the realization of a broad emission spectrum without any gap. An alternate design scheme, in which the material composition of all the cores in a broadband QCL is kept constant, is therefore desirable, provided high efficiency can be maintained at all wavelengths.

To address this issue, a new design approach was put forward where the compositions of highly strained $Al_{0.63}In_{0.37}As/Ga_{0.35}In_{0.65}As$ were kept constant, while the net strain in the structure can be tuned by using composite wells of $Ga_{0.35}In_{0.65}As/Ga_{0.47}In_{0.53}As$ [29]. For a MBE system with reasonable flux stability, a number of QCL wafers designed at different wavelengths can be grown one after another before the need for calibration. This significantly reduces the time and effort for a QCL growth facility, which in turn reduces the cost per wafer.

Figure 4(a) shows the schematic of the heterogeneous broadband QCL with 6 cores cascade together. Each of these cores are optimized based on similar strain balanced $Al_{0.63}In_{0.37}As/Ga_{0.35}In_{0.65}As/Ga_{0.47}In_{0.53}As$ superlattices, as shown in Fig. 4(b). The maximum wall plug efficiencies are 18.4%, 15.7%, 15.4%, 13.2%, 4.8% for 5.2, 6.7, 8.2, 9.1, 11 μm, respectively. These values are comparable to the state-of-the-art. The EL and emission spectrum of the lasers just beyond threshold are shown in the Fig. 5(a). Emission covering a range of 1014 cm^{-1} is observed, making them suitable for integration into a heterogeneous broadband laser.

A heterogeneous QCL active region, containing 6 optimized sub-cores, was designed for emission between 6 and 10 μm. All the sub-cores are based on the similar composite well scheme. Single mode DFB emission between 5.9 and 10 μm was obtained in the first attempt (Fig. 5(b)). Although there is insufficient gain in between the subpeaks, it can be addressed by changing the number of emitting stages, the relative arrangement, and the emission wavelength of the sub-cores, to achieve a flat gain.

#229245 - $15.00 USD Received 8 Dec 2014; revised 7 Jan 2015; accepted 27 Jan 2015; published 25 Mar 2015

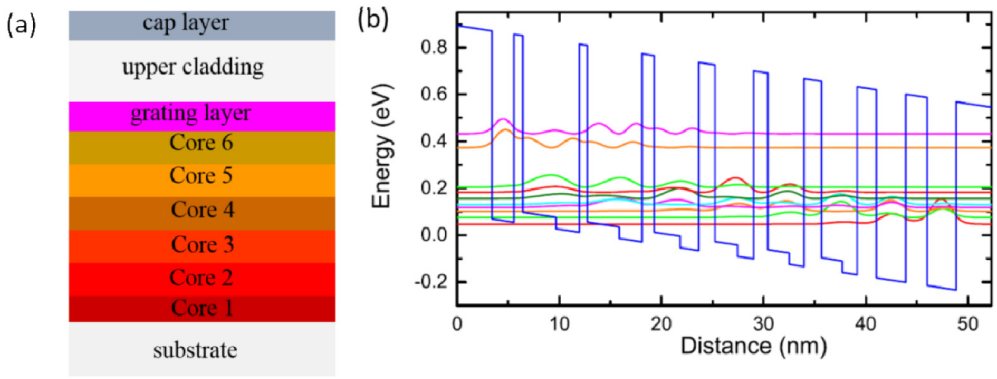

Fig. 4. (a) Schematic of the heterogeneous broadband QCL. (b) Structure of an 8.2μm QCL.

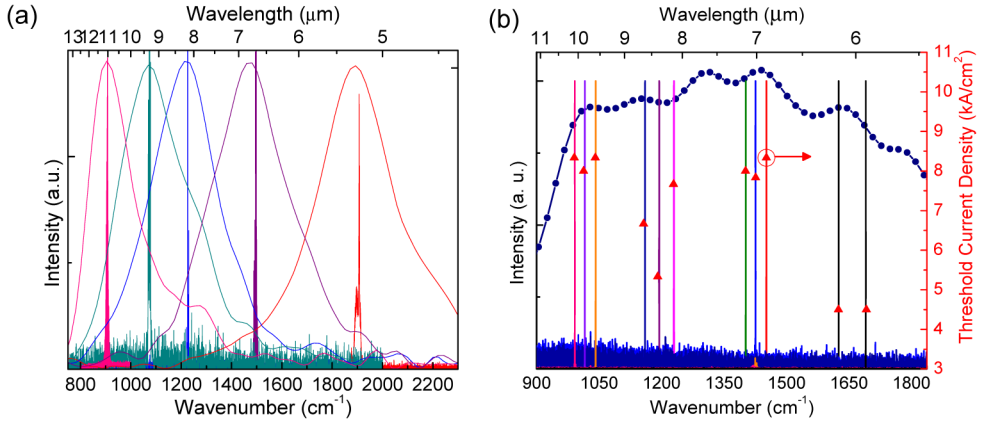

Fig. 5. (a) Electroluminescence and laser emission spectrum of the separate composite well QCLs. (b) EL and DFB spectra, along with the DFB threshold current densities of the broadband QCL.

5. Wavelength agile quantum cascade lasers

The quantum cascade laser is a powerful tool for spectroscopy. The wide spectral coverage, combined with narrow linewidth output and high power enable a wide variety of applications, including photoacoustic and standoff spectroscopy. However, conventional narrow linewidth QCLs have a tuning range of only ~5 cm^{-1}, which typically limits detection to a single type of molecule. External cavity technology can significantly expand the tuning range, but the requirement of precision optics, susceptibility of this system to mechanical vibrations, and limited scan speed due to large grating mass limits the technological potential.

As an alternative, we have adapted sampled grating distributed feedback (SGDFB) technology for fully monolithic, electronic tuning of the QCL (Fig. 6(a)) [30]. Similar technology was originally developed for telecommunications and more recently applied to quantum cascade laser by our team. In the SGDFB laser, two sampled grating sections, with different sampling period are combined within the same waveguide. Changing the current density in one section relative to another (ΔJ) changes the emission wavelength via the Vernier effect. In principle, a large (>10 ×) tuning range enhancement is possible over standard single mode lasers with proper design.

#229245 - $15.00 USD Received 8 Dec 2014; revised 7 Jan 2015; accepted 27 Jan 2015; published 25 Mar 2015

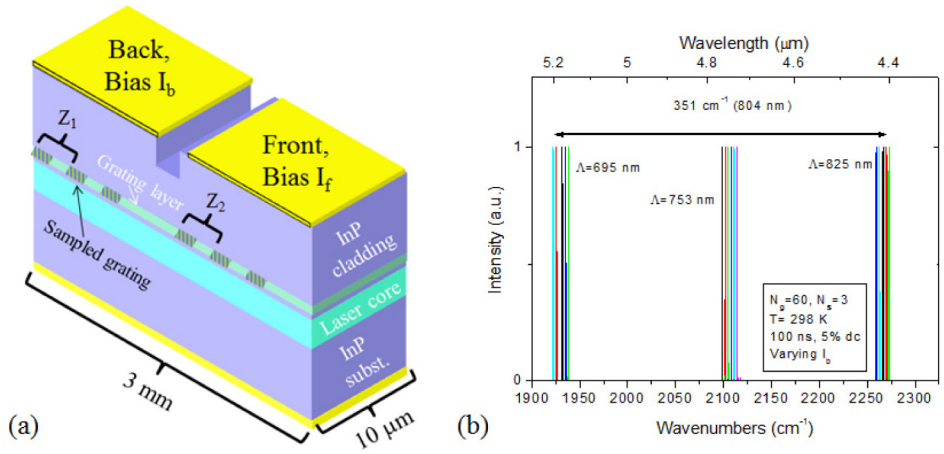

Fig. 6. (a) Schematic diagram of the SGDFB geometry. (b) Spectral coverage achieved with discrete SGDFB lasers with different grating periods on a single wafer.

A SGDFB QCL with front and rear section lengths of ~1.6 mm and ~1.4 mm was fabricated. Both sections use 30 period gratings which are sampled 3 times, where the grating period is 753 nm. The wafer is processed into a double channel ridge waveguide with ridge width of 10μm and cleaved into a device cavity length of 3 mm. Single mode tuning of more than 50 cm^{-1} is obtained above threshold by increasing the current in one section. This is a 5-10 times increase over the electrical tuning of a simple DFB laser. More than 100 mW of CW power, with a mean SMSR of 24 dB is obtained at RT over the tuning range.

After SGDFB operation was demonstrated near the gain peak, the next area explored was the overall spectral range achievable on a given wafer. The laser gain region used for the SGDFB experiment has an electroluminescence full width at half maximum (FWHM) of 400 cm^{-1} at room temperature. Only ~120 cm^{-1} around the center of the gain peak was explored. Demonstrating a single mode laser emitting far from the laser gain peak is more difficult, however, as we must provide enough gain for the cavity supermode (far from the gain peak) while suppressing the natural Fabry-Perot (FP) oscillation (at the gain peak).

With the application of anti-reflective (AR) coatings (10% on both facets), the SGDFB technology was shown to allow discrete laser to emit over a wide spectral range on a single wafer. In order to compensate for this reduced feedback, the number of grating periods per sampling period was increased to 60. To determine the full spectral range of this design, additional testing of N_g = 60 lasers with grating periods of 695, 753, and 825 nm are shown in Fig. 6(b). The pulsed threshold current ranges from 0.6 A near the gain peak to 0.9 A at the extreme of the spectral coverage. A similar single interval tuning range (16 cm^{-1}) is demonstrated for all three lasers. In total, over 800 nm (351 cm^{-1}) is shown to be accessible with single mode behavior for this SGDFB design. The peak power level of the Λ = 753 nm laser ranges from 380 to 1200 mW across its tuning range [31].

#229245 - $15.00 USD Received 8 Dec 2014; revised 7 Jan 2015; accepted 27 Jan 2015; published 25 Mar 2015

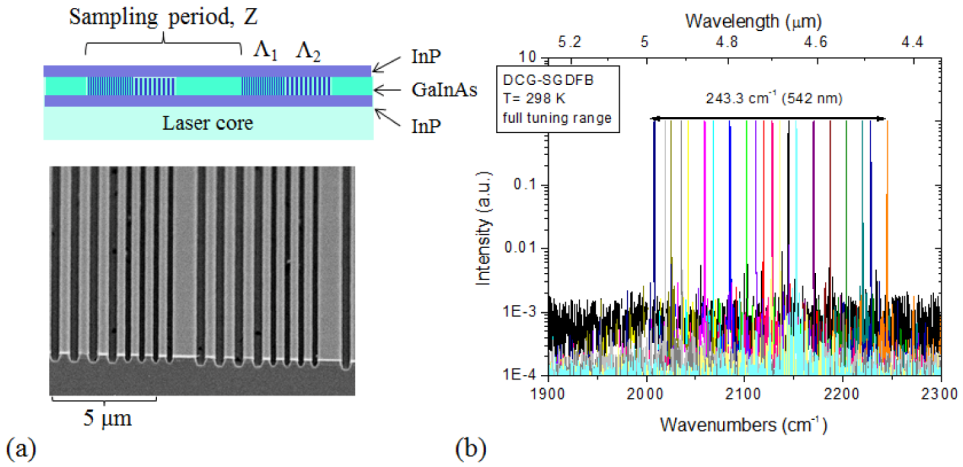

Fig. 7. (a) Schematic diagram of a digital concatenated grating and an oblique image of a etched dual grating test piece. (b) Selected emission spectra from a tunable DCG-SCGDFB operating at room temperature.

The tuning range of individual SGDFB lasers has also been further explored with the use of more advanced grating structures. The main challenge is overcoming the peaked nature of the gain curve. This was achieved by modifying the diffractive feedback within the laser cavity to partially compensate for the curvature of the gain spectrum. A digital concatenated grating (DCG) was employed for this purpose. A DCG consists of multiple sampled gratings (2, in this case) with different Bragg wavelengths and the same sampling period. A schematic of this structure and an experimental realization are shown in Fig. 7.

To experimentally demonstrate wide electrical tuning, a laser was fabricated using the DCG-SGDFB design principle. Dual sampled gratings with periods of Λ_1 = 670 and Λ_2 = 920 nm were employed to cover a wide spectral range. In order to provide a wide tuning range and sufficient feedback, the number of grating periods per sampling period was significantly reduced (4 of each grating period) and the number of sampling periods was increased (25 per section). In total, 9 mm cavities were fabricated with AR coatings. This method did prove successful, allowing up to 243 cm^{-1} of tuning for a single laser emitting near λ = 4.6 μm [32].

SGDFB QCL technology is currently being explored for even wider tuning ranges. With ~200 cm^{-1} or higher tuning per laser, small format SGDFB arrays have the potential to cover extremely wide spectral regions. The main limitation is the gain bandwidth of the laser itself. Realization of wider tuning laser systems using broadband, heterogeneous lasers is currently under development.

6. QCLs with on-chip beam combining for wide electrical tuning

The recently demonstrated broadband QCL with wide wavelength coverage of 5.9- 10 μm represents an important step toward to compact and widely tunable mid-IR lasers source system. The next step is to build a proper tuning system to access this wide wavelength range. While external cavity QCLs have been able to cover a maximum 432cm^{-1} tuning from 7.6-11.4 μm [28], and DFB QCL array have shown coverage up to ~100 cm^{-1} [33], both of these two tuning systems are complicated, and rely on extra optical components for tuning or beam combination. Since each element in the DFB array can only tune over a small range of a few cm^{-1}, the size of the array could be prohibitively large in order to cover a range of hundreds of cm^{-1}. Using sampled grating distributive feedback (SGDFB) QCL as the element of a tunable laser array would significantly reduce the number of elements in the array for the same tuning range. In addition, as the number of elements is small, an on-chip beam combiner can be integrated to route the signal from different SGDFB lasers into a single output channel.

#229245 - $15.00 USD Received 8 Dec 2014; revised 7 Jan 2015; accepted 27 Jan 2015; published 25 Mar 2015

The functionality of an on-chip beam combiner for QCLs has been demonstrated with a tree-array combiner for power scaling [34].

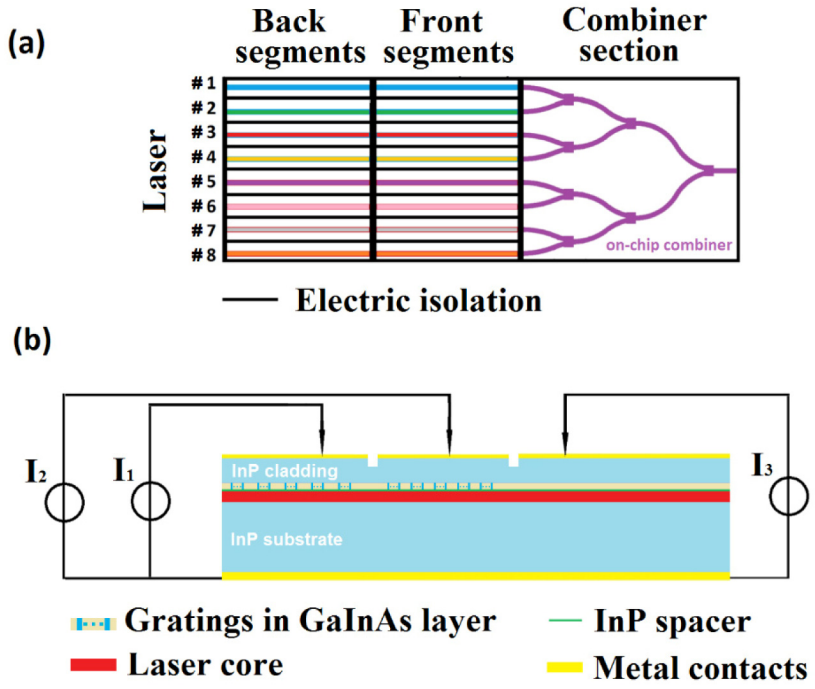

Fig. 8. (a). The schematic diagram of the three section QCL source, which contains eight SGDFB lasers and a tree-array beam combiner section. (b). The laser structure and the three section independent biasing scheme.

In our recent work, we demonstrate the first tunable QCL array with an on-chip beam combiner. The laser source is able to access a gapless tuning range of 181.7cm^{-1}, covering a wavelength range from 6.73 to 7.66 μm [35]. The tunable QCL array consists of eight two-section SGDFB QCLs with a beam combiner, as shown in Fig. 8. The combiner section contains seven identical two-in-one combiners that route the eight laser inputs to a single output in a tree-array fashion. Two segments from one common laser and the combiner section can be independently biased for device operation. The total number of contacts is 17, excluding the shared bottom contact.

In the best working condition, the combiner section can be biased as an optical amplifier, so that splitting losses can be compensated and high power output can be achieved simultaneously. Optimizing the combiner for efficient amplification and beam quality is currently being investigated. Once this technique is applied to a laser with a broad and flat gain medium, a monolithic, widely tunable QCL source is anticipated.

7. THz sources based on DFG in mid-IR QCLs

The THz spectral range (1-10 THz) is extremely interesting for applications such as explosive and drug detection, security screening (T-ray imaging), astronomy, and medical imaging. Many of these applications have the potential to impact (and safeguard) our daily lives, and, as such, have a tremendous appeal to the general public and industry. As telecommunication technology has demonstrated over the past 30 years, monolithic integration is the next logical step in pushing THz technology closer to an ideal source. Wafer scale processing allows for mass production with high yield and low cost. Toward this end, development of both component and integration technologies are critical.

#229245 - $15.00 USD Received 8 Dec 2014; revised 7 Jan 2015; accepted 27 Jan 2015; published 25 Mar 2015

One promising platform is InP-based intracavity difference frequency generation using mid-IR quantum cascade lasers (QCLs) [36–38]. This technique combines a dual frequency pump laser with engineered intersubband nonlinear susceptibility ($\chi^{(2)}$) to generate narrow linewidth THz radiation inside a single waveguide. Besides providing a wealth of beautiful physics to study, this technique allows for compact, room temperature operation over a wide spectral range. Our group, utilizing state-of-the-art QCL technology, is making steady progress in this field in the following four aspects: stable THz frequency emission; high THz power; continuous wave operation; and wide frequency tenability [39].

In a typical multimode Fabry-Pérot (FP) cavity, the light intensity spreads out among different mid-IR frequencies, and the total power is the sum over many small W_i components. As such, the product W_iW_j will be small and the THz spectrum will be rather broad (Δv ~0.5-1 THz). In order to purify and tune the THz spectrum, all the mid-IR power needs to be concentrated on the two mid-IR frequencies with single mode operation, and their frequency positions need to be controllable and tunable. The most straightforward way to this end is to use the composite DFB grating with two wavelength components, as shown in Fig. 9(a), to purify and tune the mid-IR spectra, and thus the THz spectra. With this technique, the first room temperature single mode THz emission with a stable frequency output and narrow linewidth at 4.1 THz with different currents and temperatures is demonstrated [38]. This lays the basis for our following work where single mode THz emission is the common feature of our THz sources.

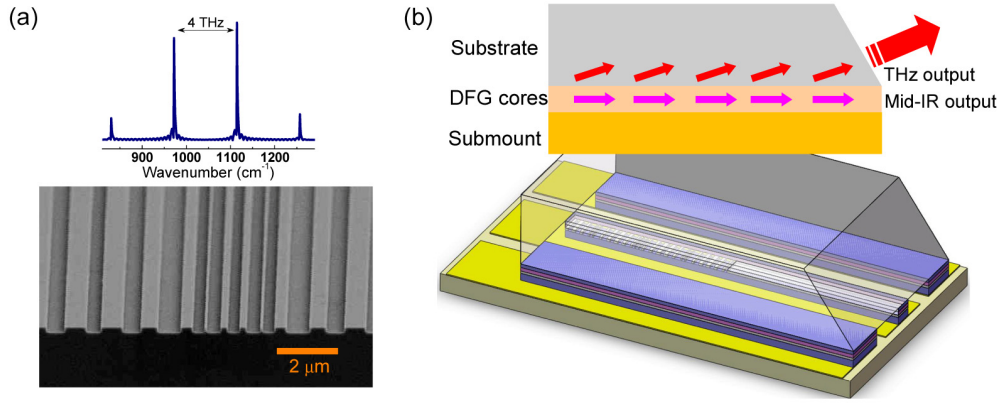

Fig. 9. (a). Composite DFB grating with two wavelength components (lower part) and its Fourier transform (upper part). (b). Schematics of Čerenkov phase matching (upper part) and epi-down mounted THz device (lower part).

The active region design for the first-generation THz QCL sources based on DFG is a dual-core structure featuring double-phonon-resonance (DPR) and bound-to-continuum (BTC) depopulation schemes for the two wavelengths. However, only the BTC core is designed with a giant nonlinear susceptibility and the DPR core merely acts as a mid-IR source with little THz generation [36,37]. To improve the nonlinear THz conversion, the second-generation THz sources feature a dual core structure with two single-phonon-resonance (SPR) designs and both are designed with a giant $\chi^{(2)}$ in the 1-5 THz range [40]. To explore the broadband THz generation of this design, an array of 10 composite DFB devices is fabricated with a modal phase matching scheme, and THz step tuning from 3.3 to 4.6 THz is achieved.

A waveguide with a modal phase matching scheme is very lossy due to high free-career absorption in the n-doped InP substrate. Because a faster frequency dependent effective index in the THz range with respect to the mid-IR index ($n_{mid\text{-}IR}$), the modal phase matching is only satisfied within a relatively narrow frequency range for a certain waveguide. To overcome this limitation, the lossy substrate can be replaced with semi-insulating InP substrate, and the

#229245 - $15.00 USD Received 8 Dec 2014; revised 7 Jan 2015; accepted 27 Jan 2015; published 25 Mar 2015

Čerenkov phase-matching scheme can be used to extract the THz light from the cavity, as shown in Fig. 9(b) [41,42]. In the Čerenkov configuration, the THz index (n_{THz}) in the QCL active region is higher than the mid-IR index, so the fundamental mid-IR wave propagates faster than the DFG THz wave. This phase matching scheme, together with the composite DFB array design allows for a wide range single mode THz generation, i.e. as wide as 1.0 to 4.6 THz was achieved (Fig. 10(c)).

Despite this wide spectral coverage, the THz power is limited, on the order of tens of μW. This is because of the poor heat removal mechanism due to the epilayer-up mounting and 350 μm thick substrate, and the inefficient current injection scheme due to the single-side current injection through a thin layer of bottom contact. To address these issues, epilayer-down mounting of the Čerenkov device on a patterned submount and double-sided current injection scheme were used [43], as shown in Fig. 9(b), and a high THz peak power of 0.22 mW was demonstrated. For this epi-down mounting strategy, thermal accumulation is greatly relieved for devices with broader area. Thus, the THz peak power in pulsed mode operation can be scaled up significantly with the mid-IR power product and conversion efficiency. Recently, the THz peak power up to 1.9 mW with conversion efficiency of 0.8 mW/W^2 was demonstrated by using this technique, as shown in Fig. 10(a) [44]. Here and after, the measured THz power is not corrected with any collection efficiency due to the improved the collection efficiency in the testing setup. The maximum WPE for this device reaches to 0.7 × 10^{-5}. Further scaling the THz power with broad-area waveguide design [45] should be able to increase the power and efficiency significantly.

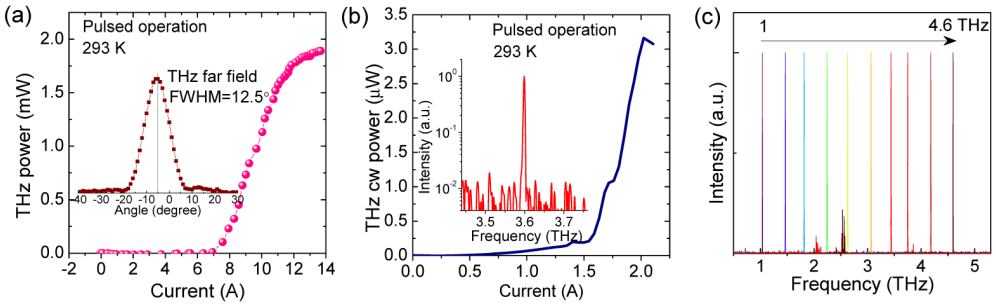

Fig. 10. Recent development of THz QCL sources with high peak power (a), continuous wave operation (b), and wide range frequency tenability (c), at room temperature.

The capability of CW THz operation at room temperature is of utter importance to wide application and commercialization. By reducing the waveguide loss with buried composite DFB grating and buried ridge waveguide, we demonstrated the first room temperature continuous wave THz QCL source with power of 3 μW at 3.6 THz (Fig. 10(b)) with epi-down mounting scheme [46]. The THz power under CW operation is expected to be improved with an better active region design and growth, as well as engineering an outcoupling scheme with higher efficiency.

The above demonstrations are single mode THz emission with a nearly fixed THz frequency output. For most of the terahertz technology applications, a compact THz source covering the entire 1-5 THz frequency range is highly desired. Towards to this end, we demonstrated a widely electrically tunable room temperature THz source with continuous frequency tuning range of 2.6-4.2 THz by using a multi-section SGDFB-DBR waveguide geometry [47]. The device consists of two SGDFB sections and a DBR section with two 100-μm isolation channel between the three sections. The two SGDFB sections were applied with different DC currents to access a wide range THz step tuning with a frequency step of 160-180 GHz. To bridge the frequency step, a quasi-continuous tuning was realized by applying different DC currents to the DBR section.

#229245 - $15.00 USD Received 8 Dec 2014; revised 7 Jan 2015; accepted 27 Jan 2015; published 25 Mar 2015

Though the current implementation is a good start, theory predicts significantly higher powers in a wider range are possible. With further development, this portable platform will one day be an enabling technology for a variety of THz research topics and applications.

8. Conclusion

The quantum cascade laser is becoming the leading semiconductor laser source in the mid-infrared and THz frequency ranges thanks to the tremendous development in the past two decades. Particularly, the recent breakthroughs in high power, high efficiency QCLs in the 3-5 μm wavelength range, surface emitting ring cavity QCL, high power β-type distributed feedback QCL, broadband QCLs with a wide spectral range of 3 to 12 μm, wavelength agile QCLs based on dual-section sampled grating design, on-chip QCL beam combiners for wide-range electrical tuning with controlled beam quality, and high performance room temperature THz QCL sources based on difference frequency generation, are pushing QCL technology to new frontiers of research. With further development of this technology, many new QCL-based applications are likely to emerge in the near future.

Acknowledgments

This work is supported by the National Science Foundation under Grant No. 1359779, 1231289, and 1306397. The authors would like to acknowledge the support, interest, and encouragement from DHS, NASA, and Navy.

#229245 - $15.00 USD Received 8 Dec 2014; revised 7 Jan 2015; accepted 27 Jan 2015; published 25 Mar 2015